Available online at www.sciencedirect.com

SCIENCE DIRECT®

International Journal of Pharmaceutics 267 (2003) 49–58

international journal of pharmaceutics

www.elsevier.com/locate/ijpharm

Investigation of structural and dynamic features of the radicals produced in gamma irradiated sulfanilamide: an ESR study

Ş. Çolak, M. Korkmaz*

Physics Engineering Department, Hacettepe University, 06532 Beytepe, Ankara, Turkey

Received 28 October 2002; received in revised form 22 July 2003; accepted 30 July 2003

Abstract

Characteristic features of the radiolytical intermediates produced in gamma irradiated solid sulfanilamide (SA) were investigated in the present work using ESR spectroscopy. SO_2, which is the most sensitive group to radiation of SA molecule, was found to be at the origin of radiation produced ionic radical species. The latters give rise to an axially symmetric and an isotropic ESR spectra so that their sum appears as a three line antisymmetric ESR spectrum. Heights of these lines measured with respect to the base line were used to monitor microwave, temperature, time-dependent and kinetic features of the radical species contributing to ESR spectrum. Based on the experimental results derived from this study, it was concluded that as in the case of other solid sulfonamides radiation, yield of solid SA is very low ($G = 0.5$) compared with those obtained for sulfonamide aqueous solutions ($G = 3.5$–5.1), so that SA and SA-containing drugs could be safely sterilized by radiation.

Keywords: Radiosterilization; Sulfonamides; Sulfanilamide; Radical kinetics; ESR

---

1. Introduction

Sulfonamides or sulfa drugs are the chemical substances derived from sulfanilamide (SA) whose chemical name is *para*-amino benzene sulfonamide. Namely, SA is the grandparent of the sulfonamide family of drugs that are still widely used today in a variety of applications including the treatment of meningitis, ulcerative colitis, urinary tract infections, and dysentery, as well as in veterinary medicine in spite of the discoveries of modern antibiotics. Sulfonamides were the first substances used to cure and prevent bacterial infections in humans. They are bacteriostatic, that is, they do not kill bacteria but inhibit growth and multiplication by interfering with their enzyme systems.

SA is used in case of bacterial inflammations of the skin and of the genital area. Therefore, it is included in eye ointments and drops; in preparations for application in case of furuncles, irritated wounds, abscesses, leg ulcers; in vaginal ointments and suppositories and in the special form of allergic contact dermatitis. Particular interest now centers on the preparation of sterile unit-dose preparations. Radiation is successfully used for the sterilization of bioproducts and pharmaceuticals (Christensen et al., 1967; Gaughran and Goudie, 1977; Jacobs, 1991; Reid, 1995; Duroux et al., 1996; Pourahmad and Pakravan, 1997; Safrany, 1997), particularly when conventional methods are inadequate. A difficulty, however, is that certain undesirable radiolytical intermediates may accompany treatment with a sterilizing dose of irradiation. No

---

* Corresponding author. Tel.: +90-312-297-72-13; fax: +90-312-299-20-37.
E-mail address: seyda@hacettepe.edu.tr (M. Korkmaz).

0378-5173/$ – see front matter © 2003 Elsevier B.V. All rights reserved.
doi:10.1016/j.ijpharm.2003.07.002

information is available, as far as we are aware, about the structural and dynamic features of these intermediates produced in irradiated solid SA which is the active ingredient of several sulfa drugs. Therefore, the aim of this work is to investigate in detail the radiosensitivity of SA and to characterize the radiolytical intermediates produced in gamma irradiated SA in the dose range of 5–50 kGy using ESR spectroscopy.

2. Materials and methods

SA or with its chemical name, 4-aminobenzenesulfonamide of spectroscopic grade was provided from Merck Company Ltd., istanbul, and was stored in dark at room temperature. No further purification was performed and it was used as it was received. SA is a light sensitive white powder slightly soluble in water and has a molecular structure given in Fig. 1. All irradiations were performed at room temperature (293 K) in dark using a ^{60}Co gamma cell supplying a dose rate of 2.52 kGy/h as an ionizing radiation source at the Sarayköy Establishment of Turkish Atomic Energy Agency in Ankara. The dose rate at the sample sites was measured by a Fricke dosimeter, and ESR investigations were performed on samples irradiated at four different doses (5, 10, 25, and 50 kGy).

ESR measurements were carried out using Varian 9″-EL-X band ESR spectrometer operating at 9.5 GHz and equipped with a TE_{104} rectangular double cavity containing a DPPH standard sample in the rear resonator which remained untouched throughout the experiment. The spectrometer operating conditions adopted during the experiment are given in Table 1. The spectra were recorded at room temperature and at different temperatures at different microwave power levels. Signal intensities were calculated from first derivative spectra and compared with that obtained for a standard DPPH sample under the same spectrometer operating conditions. Sample temperature inside the microwave cavity was monitored with a digital temperature control system (Bruker ER 4111-VT). The latter provided the opportunity of measuring the temperature with an accuracy of ±0.5 K at the site of the sample. A cooling, heating, and subsequent cooling cycle was adopted to monitor evolutions of the free radical signals. The temperature of the samples was first decreased to 120 K starting from room temperature with an increment of 20 K, then increased to 400 K, and finally was decreased again to room temperature.

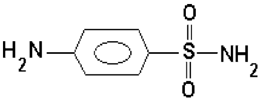

Fig. 1. Molecular structure of SA.

Table 1
ESR spectrometer operating conditions adopted throughout the experiment

Central field	327.5 mT
Sweep width	10 mT
Microwave frequency	9.26 GHz
Microwave power	1 mW
Modulation frequency	100 kHz
Modulation amplitude	0.1 mT
Receiver gain	1.25×10^3 to 5×10^2
Scan time	240 s
Time constant	1 s
Temperature	110–400 K

Kinetic studies of the contributing free radicals were also performed at different temperatures. To achieve this goal, the samples were heated to predetermined temperatures (323, 348, 365, 378, 393, and 413 K) and kept at these temperatures for predetermined times (3, 8, 13, 20, 40, 70, 100, and 160 min), then they were cooled to room temperature and their ESR spectra were recorded. The results were the average of five replicates for each radiation dose. Signal intensity variation data obtained for different annealing temperatures were used to characterize the contributing radiation-induced free radicals.

Digitized signal intensity data derived from room temperature ESR spectrum of a sample irradiated at dose of 25 kGy were used as input for simulation calculations basing on a model of two radical species of different spectroscopic features.

3. Experimental results and discussion

3.1. Room temperature study

Although unirradiated SA exhibited no ESR signal, irradiated SA showed a very simple ESR spectrum consisting of three resonance lines appearing

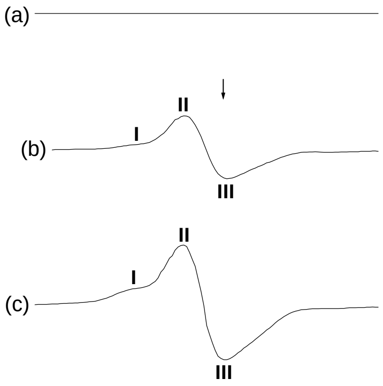

Fig. 2. Room temperature ESR spectra of SA. (a) Unirradiated (control) and irradiated at the dose of (b) 10 kGy, (c) 50 kGy. Arrow indicates the position of DPPH line.

Table 2
Theoretical functions best fitting to microwave saturation data

Line	Functions
I	$f(\text{I}) = 74.22(1 - e^{-0.34\sqrt{P}})$
II	$f(\text{II}) = 77.19(1 - e^{-1.28\sqrt{P}})$[a] $f(\text{II}) = -273.46 + 358.50\, e^{-0.012\sqrt{P}}$[b]
III	$f(\text{III}) = 84.99(1 - e^{-1.01\sqrt{P}})$[a] $f(\text{III}) = 73.37 + 196.70\, e^{-0.81\sqrt{P}}$[b]
Standard	$f(\text{s}) = 439.38(1 - e^{-0.09\sqrt{P}})$

P, microwave power in mW.

[a] Increasing part.

[b] Decreasing part.

at g values of 2.0089, 2.0060, 2.0038 as given in Fig. 2b and c with their assigned line numbers. Increase in absorbed dose did not create any pattern change in the room temperature spectra. Variations of the peak heights, measured with respect to base line, of these resonance lines with applied microwave power were studied first. The results of this study, presented in Fig. 3, indicate that at least two radical species of different saturation characteristics were involved. Although line I saturates as an inhomogeneously broadened line, lines II and III saturate as homogeneously broadened resonance lines. Theoretical functions best fitting to microwave saturation data were also derived. The results of this calculation are summarized in Table 2. As for variations of the peak heights of I, II and III resonance lines with absorbed radiation dose, it was found that they follow the sum of two curves of the type $f_1 = bD$ and $f_2 = f_0(1 - e^{-aD})$ in the dose range of 0–50 kGy (Fig. 4).

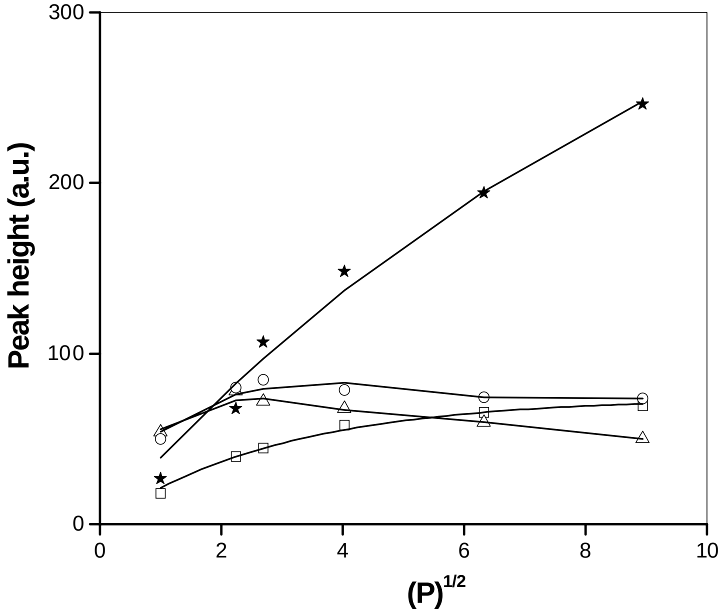

Fig. 3. Variations of ESR peak heights vs. square root of applied microwave power (P) for a sample irradiated at a dose of 25 kGy. (□) line I, (△) line II, (○) line III, (★) standard. Solid lines represent theoretical curves best fitting to experimental data.

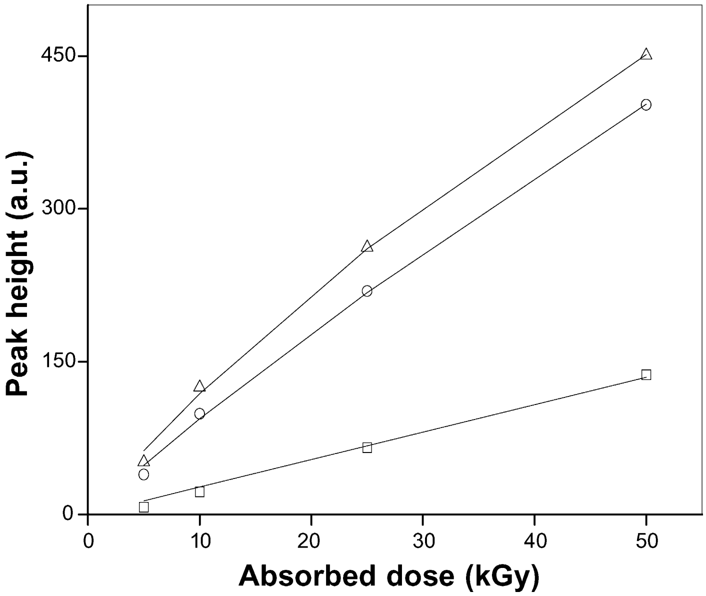

Fig. 4. Variations of peak heights with absorbed radiation dose. (□) line I, (△) line II, (○) line III. Solid lines represent theoretical curves best fitting to experimental data.

In these expressions D stands for the absorbed dose in kGy. Functions and parameters best fitting to experimental dose–response curves are presented in Table 3.

3.2. Variable temperature study

Variations of the peak heights with temperature in the range of 290–400 K were also studied. The results are given in Fig. 5. The increase in temperature produced practically no changes in the peak heights of the resonance lines I, II, and III up to 320 K. However, warming the sample above this temperature caused continuous decrease in the peak heights of the resonance lines II and III, but it created a slight increase in the height of line I, up to 375 K, then a relatively sharp decrease occurred. Observed changes in the heights of all resonance lines were found to be irreversible. This fact indicates that radiation-induced radicals giving rise to observed resonance lines decay at high temperatures. Cooling the sample down to room temperature did not create any pattern change in the spectra, except slight reversible increases in the peak heights. Microwave saturation features of the resonance lines at 110 K were also studied and similar behaviors to those obtained at room temperature were observed.

Table 3
Functions and parameters best fitting to experimental dose–response data

Line	Functions
I	$f'(\mathrm{I}) = 2.69D + 0.1(1 - \mathrm{e}^{-0.047D})$
II	$f'(\mathrm{II}) = 6.34D + 148.60(1 - \mathrm{e}^{-0.047D})$
III	$f'(\mathrm{III}) = 6.78D + 70.35(1 - \mathrm{e}^{-0.047D})$

D stands for absorbed dose in kGy.

3.3. Radical decays in annealed samples

The radical species responsible for three lines ESR spectra observed for irradiated SA are expected to have different decay characteristics depending on the sample temperature. The decay rates of the radicals at high temperature should be higher than the decay rates at low temperatures. In fact, it was found that it is the case. Radiation-induced radicals in SA were observed to be very unstable even at room temperature irrespective of irradiation dose (Fig. 9). Increase in temperature accelerated the decay and thermal creation of the radicals, and the higher the temperature the higher the decay and creation rates of the radicals. Signal

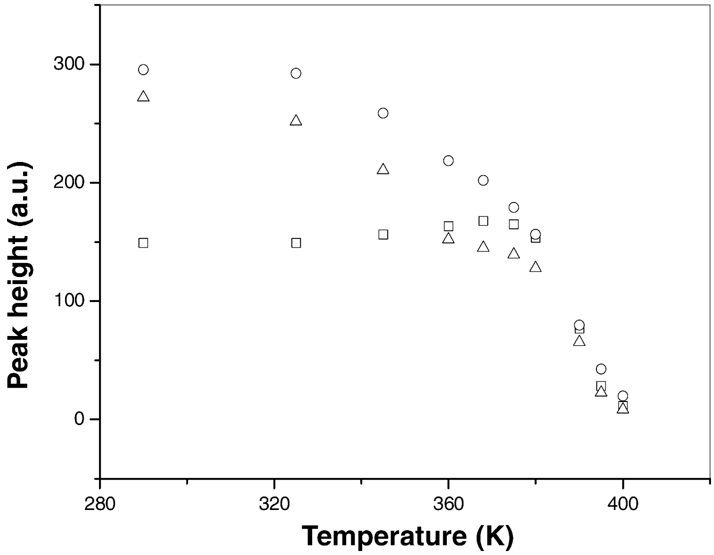

Fig. 5. Variation of peak heights with temperature. (□) line I, (△) line II, (○) line III.

intensity decay results obtained for SA samples irradiated at a dose 25 kGy and annealed at different temperatures for different times are summarized in Figs. 6–8. As seen from these figures, kinetic behaviors of the contributing radicals are very different. Although the height of line I increases at annealing temperatures of 323 and 348 K, lines II and III tend to decrease at these temperatures. This shows, once more, the difference

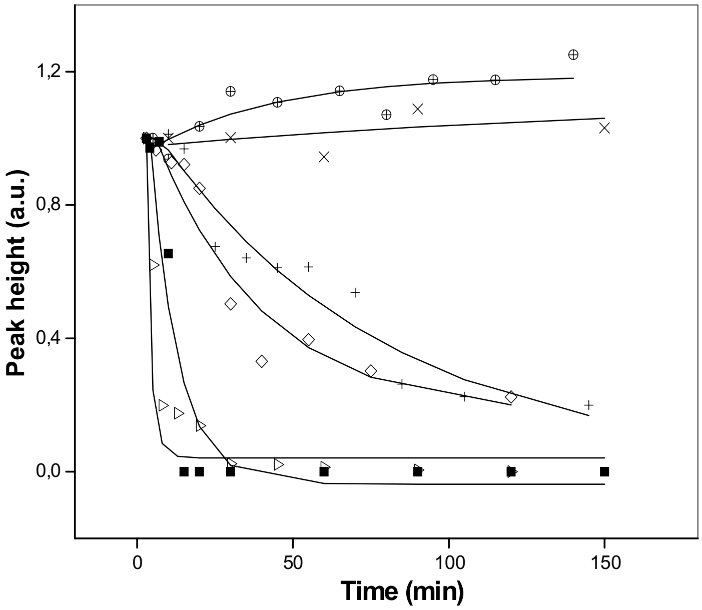

Fig. 6. Signal intensity decay results for line I of a sample irradiated at a dose of 25 kGy and annealed at six different temperatures (×: 323 K, ⊕: 348 K, □: 365 K, +: 378 K, ▹: 393 K, ■: 413 K) for different times.

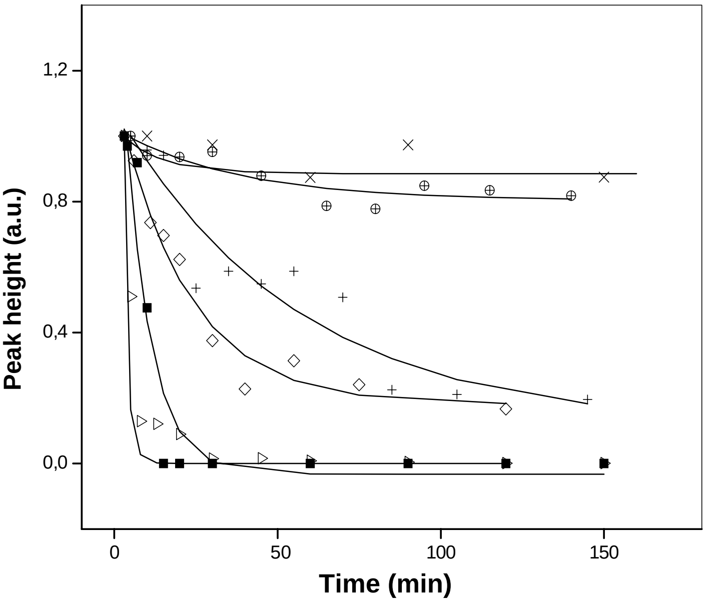

Fig. 7. Same as Fig. 6 for line II.

in thermal behavior of the responsible radicals. All lines suffer drastic intensity decrease above 365 K, and the longer the annealing time the higher the intensity decrease.

The increases in intensity of line I at the annealing temperature of 323 and 348 K (Fig. 6) originate from the fact that thermally created radicals of similar characteristics to those produced by radiation overcome

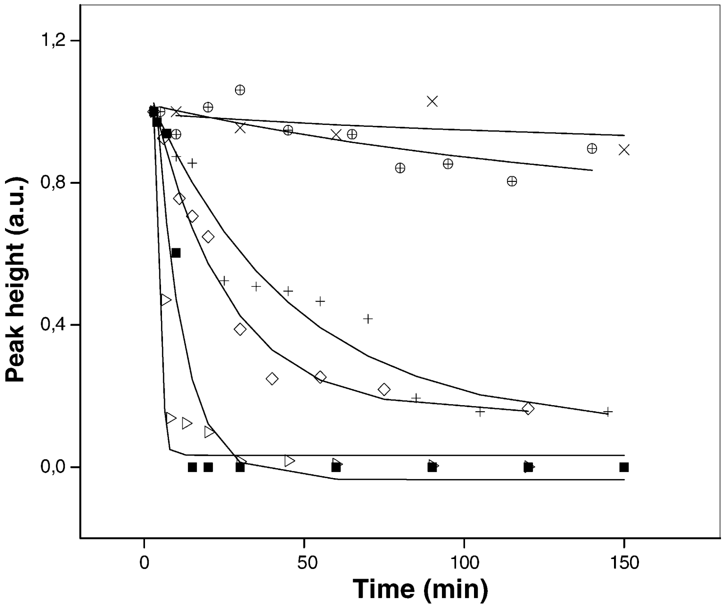

Fig. 8. Same as Fig. 6 for line III.

the slight radical decay occruing at these temperatures. However, this is not the case for lines II and III and they always decay at high temperatures. It is difficult to determine the decay characteristics of the contributing radicals from high temperature kinetic study data due to the fact that: first, resonance lines are not single but overlapping ones and second, the decay and thermal radical creation compete above room temperature.

3.4. Proposed radical species

SO_2 is the most sensitive group to radiation in SA molecule due to its high electrophilic feature. Therefore, radicals with unpaired electrons localized on S atoms is expected to be likely produced upon irradiation as in the case of sulphur containing compounds (Samoilovich and Tsinober, 1970; Bershov et al., 1975; Huzimura, 1979; Katzenberger et al., 1989; Barbas et al., 1992; Kai and Miki, 1992; Walther et al., 1992). As in the present work, these radicals do not exhibit hyperfine structure, but they have g tensor of orthorhombic symmetry with an average value varying between 2.0037 and 2.0059 (Samoilovich and Tsinober, 1970; Bershov et al., 1975; Huzimura, 1979). Experimental g values determined in the present work for resonance lines I ($g_{\mathrm{I}} = 2.0089$), II ($g_{\mathrm{II}} = 2.0060$) and III ($g_{\mathrm{III}} = 2.0038$) stay in this range.

We believe, accordingly, that the molecular ionic fragment

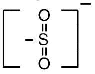

$$\left[-\overset{\overset{\displaystyle O}{\|}}{\underset{\underset{\displaystyle O}{\|}}{S}}\right]^-$$

(hereafter radical A) and $SO_2{}^-$ ionic radical (hereafter radical B) are the responsible units from the three line ESR spectra of irradiated SA. The unpaired electron in $SO_2{}^-$ ionic radical occupies the antibonding 2b* orbital formed from p orbitals of the S atom. Radicals A and B produced in irradiation powder SA are randomly oriented and the motion of radical A is restricted in large extent due to the big group attached to it, so that it gives rise to powder ESR spectra with principal g values varying between $g_{xx} = 2.0022$–2.0031, $g_{yy} = 2.0015$–2.0098 and $g_{zz} = 2.0058$–2.0066 (Bershov et al., 1975; Huzimura, 1979). As for radical B ($SO_2{}^-$ ionic radical), it has a high motional freedom, consequently, it gives rise to a single resonance line of average spectroscopic g factor varying between 2.0037 and 2.0059 (Samoilovich and Tsinober, 1970; Huzimura, 1979).

3.5. Room temperature long-term stability of the radiation-induced radicals

Room temperature stabilities of the radical or radicals in an irradiated drug or drug raw material is as important as the radiosensitivity of these materials. Therefore, this feature of the radicals produced in irradiated SA is also studied. Samples irradiated at different radiation dose levels were used to achieve this goal. Stability at room temperature of the radicals are found to be independent from the irradiation dose. The signal intensity decay data obtained for a sample irradiated at a dose of 25 kGy were used to get the decay characteristics of the contributing radicals. The data relative to the variations of signal height of different resonance lines over a period of 90 days are given in Fig. 9. A slight increase in the height of line I in the beginning of storage period was the common behavior of the samples irradiated at different doses and stored at room temperature. This likely originates from the transformation of the radicals dominating lines II and III to the radical giving rise to line I. However, as it is seen from Fig. 9 the extent of this transformation is relatively small.

Signal height decay data of lines II and III were found best fitting to two different exponential functions of different weights and of different decay constants. This justifies, once more, that two radical species of different decay characteristics contribute to the ESR spectra of irradiated SA. The results of this calculation are summarized in Table 4.

3.6. Simulation of room temperature ESR spectra

Room temperature experimental signal intensity data obtained from the ESR spectrum of a sample irradiated at a dose of 25 kGy were used as input

Table 4
Relative weights and decay constants of the contributing radicals calculated from room temperature long-term signal intensity decay data

Line	Radical species	Relative weight	Decay constants (day^{-1})	r^2
II	A	48.11 (±19.65)	0.00053 (±0.00002)	0.975
	B	201.64 (±20.49)	0.14487 (±0.03659)	
III	A	70.84 (±6.27)	0.00053 (±0.00002)	0.943
	B	155.24 (±13.02)	0.14487 (±0.03659)	

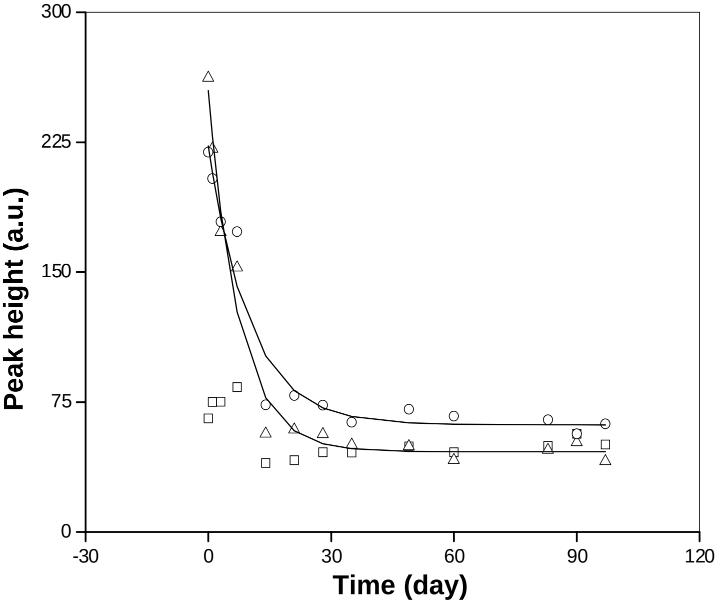

Fig. 9. Variations in signal heights over a period of 90 days for SA irradiated at a dose of 25 kGy. Symbol: experimental (□: line I, △: line II, ○: line III). Solid lines: theoretical.

to perform simulation calculations. A model of two radical species was adopted throughout the calculations. Spectral parameter values determined by this technique for contributing radical species are given in Table 5. Although the line width of radical B ($SO_2{}^-$ ionic radical) is small, it dominates ESR spectrum and radical A (a molecular ionic fragment 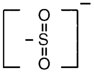 $\left[-\overset{\mathrm{O}}{\overset{\|}{\underset{\underset{\mathrm{O}}{\|}}{\mathrm{S}}}}\right]^{-}$ ϕ) contributes mainly to the line centered at $g = 2.0089$. Theoretical ESR spectrum calculated using parameter values given in Table 5 and corresponding experimental counterpart are presented together in Fig. 10. As seen, the agreement between experimental and theoretical spectra is fairly good which indicates that the model based on two radical species explains very well the experimental ESR spectra of irradiated SA.

Table 5
Calculated spectral parameters for contributing radical species

Radical species	Relative weight	Line width (*G*)	*g* factor
A	7.32	2.43	$g_{\|\|} = 2.0089$ $g_{\perp} = 2.0035$
B	226.47	1.59	$g_{\mathrm{av}} = 2.0052$

Gamma irradiated frozen aqueous solutions of sulphacetamide (50%) have been examined in the literature (Philips et al., 1971) using ESR to look for possible intermediates in the radiation degradative pathway. The examination has been conducted at 77 K and a single resonance line centered at $g = 2.0075$ was reported for a sample annealed to 120 K. This value falls into the *g* value range reported in the present work for gamma irradiated solid SA.

A *G* value (the number of radical species produced by the absorbed radiation per 100 eV) of 0.5 was obtained for gamma irradiated solid SA in this work. This value is fairly small compared with those reported for sulfonamide aqueous solutions (3.5–5.1) but stay in the range of the *G* values reported for solid sulfonamides (0.15–0.6) (Philips et al., 1971, 1973). This difference in *G* values is believed to have originates from hydrated electrons (e^-_{aq}) and hydroxyl radicals ($^\bullet$OH) produced in large amount as radiolytical intermediates in irradiated aqueous solutions of sulfonamides. These results are indicative that the SA could be radiation sterilized in the solid state.

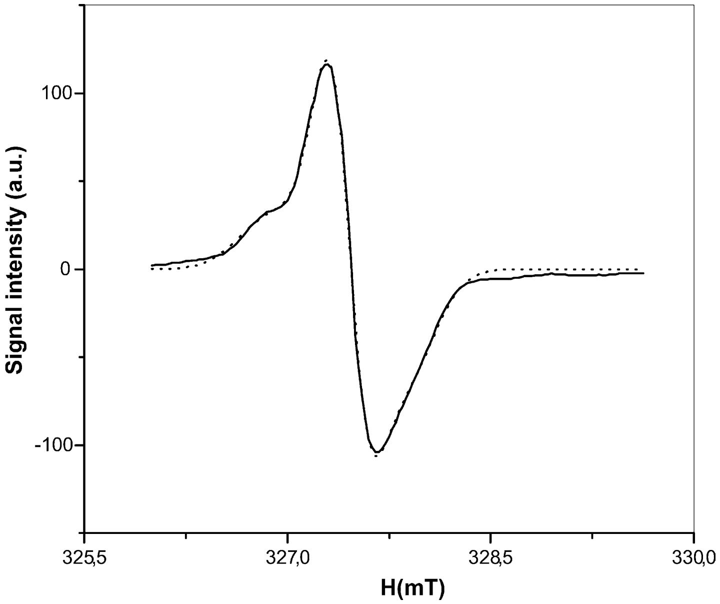

Fig. 10. Experimental and calculated ESR spectra for SA irradiated at a dose of 25 kGy. Solid line: experimental; dashed line: theoretical.

4. Conclusion

Two radicals of different spectroscopic and thermal features are produced in gamma irradiated solid SA. SO_2, which is the most sensitive subgroup to radiation in SA molecule, is shown to be at the origin of the observed three line ESR spectra. Ionic radicals

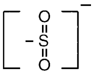
$\left[-\overset{\overset{\displaystyle O}{\|}}{\underset{\underset{\displaystyle O}{\|}}{S}}\right]^{-}$

and $(SO_2)^-$ are produced upon irradiation and they give rise to axially symmetric and isotropic ESR spectra, respectively. But the amount of these radicals in irradiated SA are not the same, and isotropic resonance line due to $(SO_2)^-$ ionic radical dominates the spectrum. Both radical species are not stable at room and especially at high temperatures (Figs. 6–8). A model based on two radical species was found to explain well the experimental results obtained for gamma irradiated SA.

As in the case of other solid sulfonamides (Philips et al., 1971, 1973), radiation yield of solid SA is very low even at the highest permitted radiation dose (25 kGy) for pharmaceutical radiosterilization and radiolytical intermediates produced in SA decay fast. This means that solid SA could not be used for sensitive dose measurement due to its poor dosimetric feature, but SA and drugs containing SA as active ingredient could be safely sterilized by radiation.

References

Barbas, M., Bach, A., Mudelsee, R., Mangini, A., 1992. General properties of the paramagnetic center at $g = 2.006$ in carbonates. Q. Sci. Rev. 11, 165–171.

Bershov, L.V., Martýrsyan, V.O., Marfunin, A.S., Speranskii, A.V., 1975. EPR and structure models for radical ions in anhydrite crystals. Fortschr. Miner. 52, 591–604.

Christensen, E.A., Holm, N.W., Juul, F.A., 1967. Radiosterilization of Medical Devices and Supplies in Radiosterilization of Medical Products. STI/PUB/157. IAEA, Vienna, pp. 265–286.

Duroux, J.L., Basly, J.P., Penicaut, B., Bernard, M., 1996. ESR spectroscopy applied to the study of drugs radiosterilization: case of three nitroimidazoles. Appl. Radiat. Isot. 47, 1565–1568.

Gaughran, E.R.L., Goudie, A.J., 1977. Sterilization by Ionizing Radiation: Sterilization of Medical Products by Ionizing Radiation, vol. II. Multiscience Publishers Ltd., Montreal, Que., Canada.

Huzimura, R., 1979. ESR studies of radical ion centers in irradiated $CaSO_4$. Jpn. J. Appl. Phys. 18, 2031–2032.

Jacobs, G., 1991. Radiation in the Sterilization of Pharmaceuticals, Sterile Pharmaceutical Manufacturing, vol. I, 1st ed. Interpharm. Press, Buffalo Groze, IL, pp. 57–78.

Kai, A., Miki, T., 1992. Electron spin resonance of sulfite radicals in irradiated calcite and aragonite. Radic. Phys. Chem. 40, 469–476.

Katzenberger, O., Debuyst, R., De Canniere, P., Dejehet, F., Apers, D., Barabas, M., 1989. Temperature experiments on mollusk samples: an approach to ESR signal identification. Appl. Radiat. Isot. 40, 1113–1118.

Philips, G.O., Power, D.M., Sewart, M.C.G., 1971. Effect of gama irradiation on sodium sulphacetamide. Radiat. Res. 46, 236–250.

Philips, G.O., Power, D.M., Sewart, M.C.G., 1973. Effect of γ-irradiation on sulphonamides. Radiat. Res. 53, 204–215.

Pourahmad, R., Pakravan, R., 1997. Radiosterilization of disposable medical devices. Radiat. Phys. Chem. 49, 2.

Reid, B.D., 1995. Gamma processing technology: an alternative technology for terminal sterilization of parenterals. PDA J. Pharmaceutic. Sci. Technol. 49, 83–89.

Safrany, A., 1997. Radiation processing: synthesis and modification of biomaterials for medical use. Nucl. Instrum. Methods Phys. Res. B 131, 376–381.

Samoilovich, M.I., Tsinober, L.I., 1970. Characteristics of radiation color centers and microisomorphism in crystals. Sov. Phys. Crystallogr. 14, 656–666.

Walther, R., Barbas, M., Mangini, A., 1992. Basic ESR studies on recent corals. Q. Sci. Rev. 11, 191–196.